

# Charge Relaxation Due to Surface Conduction on an Insulating Sheet Near a Grounded Conducting Plane

Kelly Robinson, *Senior Member, IEEE*

**Abstract**—Electrostatic charges are responsible for a variety of problems in industrial processes and customer equipment that use webs or sheets. Problems include particle contamination from attracting dust, sheets that stick to each other, and electrical discharges resulting in logic resets or damage to electrical components. These problems can be mitigated by increasing the surface conductivity of the insulating sheets by coating the surface with a conductive layer or by increasing the relative humidity. To mitigate problems, electrostatic charge must dissipate quickly compared with the mechanical transport time of the process. Reported here are the results of a model calculation of the charge relaxation time showing explicitly that the charge relaxation time depends on both surface conductivity and geometry. The charge relaxation time is found to increase as the distance to a nearby, grounded conducting plane decreases. Charge relaxation is slowed because the tangential electric field needed to drive surface current becomes smaller as the distance to the grounded plane decreases. Inferred from this analysis is the dependence of charging on the electric Reynolds number (ratio of the electrical charge relaxation time to the mechanical transport time). Web charging can be divided into three regimes: dissipation ( $R_e < 0.1$ ), transition ( $0.1 < R_e < 10$ ), and charging ( $10 < R_e$ ). Only in the transition regime does charging depend strongly on surface conductivity and speed.

**Index Terms**—Boundary condition, charge relaxation, electric field, electric potential, electric Reynolds number, insulating sheet, insulating web, Laplace equation, surface conductivity.

## NOMENCLATURE

$A$	Constant coefficient in the solution (A1) to the Laplace equation ( $\sqrt{V}$ ).
$B$	Constant coefficient in the solution (A1) to the Laplace equation ( $\sqrt{V}$ ).
$C$	Constant coefficient in the solution (A1) to the Laplace equation ( $\sqrt{V}$ ).
$D$	Constant coefficient in the solution (A1) to the Laplace equation ( $\sqrt{V}$ ).
$d$	Distance between a sheet and a nearby grounded plane above the sheet (m).
$g$	Distance between a sheet and a nearby grounded plane below the sheet (m).
$J_x$	Surface current density (A/m) in Fig. 5.
$L$	Characteristic length (m), size of a sheet or span length between conveyance rollers.

Paper MSDAD-A-04-14, presented at the 2002 Industry Applications Society Annual Meeting, Pittsburgh, PA, October 13–18, and approved for publication in the IEEE TRANSACTIONS ON INDUSTRY APPLICATIONS by the Electrostatic Processes Committee of the IEEE Industry Applications Society. Manuscript submitted for review October 15, 2002 and released for publication June 23, 2004.

The author is with Eastman Kodak Company, Rochester, NY 14652-4317 USA (e-mail: Kelly.Robinson@Kodak.com).

Digital Object Identifier 10.1109/TIA.2004.834134

$n$	Integer in the range $(0, \infty)$ .
$P$	Constant coefficient in the solution (A1) to the Laplace equation (V).
$R$	Constant coefficient in the solution (A1) to the Laplace equation (V/m).
$S$	Constant coefficient in the solution (A1) to the Laplace equation (V/m).
$T$	Constant coefficient in the solution (A1) to the Laplace equation ( $V/m^2$ ).
$t$	Time (s).
$R_e$	Electric Reynolds number defined in (1) (dimensionless).
$U$	Speed (m/s).
$x$	Distance coordinate in the plane of the web (m).
$\Delta x$	Length of a web element (m) in Fig. 5.
$z$	Distance coordinate normal to the web surface (m).
$\alpha$	Constant ( $m^{-1}$ ) in the solution (A1) to the Laplace equation.
$\epsilon_0$	Permittivity of free space; $8.854 \times 10^{-12}$ (F/m).
$\epsilon_1$	Permittivity of web or sheet material (F/m), taken to be approximately $3\epsilon_0$ .
$\Phi$	Electric potential (V).
$\rho_0$	Sheet resistivity ( $\Omega/\square$ ).
$\rho_{s,0}$	Initial uniform charge density ( $C/m^2$ ) defined in (A18).
$\sigma_s$	Sheet conductivity (S) or ( $\Omega^{-1}$ ).
$\tau^e$	Charge relaxation time (s).
$\tau^m$	Mechanical transport time (s).
$\tau_n$	Time constant (s) defined in (11) and (A22).
$\Psi$	Stream function (V).

## I. INTRODUCTION

**E**LECTROSTATIC charges are responsible for a variety of problems in industrial processes and consumer products that use webs or sheets. Problems include particle contamination from attracting dust, sheets that stick to each other causing jams or double feeds, and electrical discharges that cause system resets in the digital control system and damage to electrical components. These problems can be mitigated by increasing the surface conductivity of the insulating sheets by coating the surface with a conductive layer or sometimes by increasing the relative humidity.

To be effective, the surface conductivity must be sufficiently high for electrostatic charge to dissipate quickly compared with the mechanical transport time of the process. During the product commercialization process, determining the required surface conductivity is complicated because charge dissipation depends on both surface conductivity and geometry.

Presented here is an analysis of an idealized geometry that clearly demonstrates this dependence. Expressions for the charge relaxation time as a function of surface conductivity and geometry provide guidance for determining the required surface conductivity for specific applications.

### A. Charged Webs and Sheets Cause Problems

When two chemically dissimilar surfaces come into contact, charge is exchanged. Webs and sheets become charged when they contact metal or polymer transport rollers [1], [2]. Charge accumulation is of particular concern in photographic film production where sparks can cause marks on light-sensitive products. Web charging depends on the line speed of a process relative to the dc resistivity of the web [3]. The charging of webs by contact with conveyance rollers can be characterized by empirical constants [4]. Pinch rollers are of particular interest because significant and destructive charging can occur in a single contact [5]. Imparting conductivity to a plastic film surface is a well-known strategy for reducing charge levels where the product of velocity and sheet resistivity is a useful scaling factor [6]. Higher conductivity is needed for processes with higher speeds [7].

Surface charge on sheets and webs can cause a variety of problems. Dirt attraction and contamination are serious concerns for the motion picture industry [6]. Receiver sheets often become charged in electrophotographic or thermal printers resulting in conveyance problems and jams [8]. Extra force is required to peel an electrostatically charged, insulating sheet from a grounded plane, which is of interest in the electrostatics of parachutes; and handling of paper and polymer sheets is of concern in the converting and textile industries [9].

### B. Surface Conductivity Mitigates Problems

Surface conductivity provides a path for charge on a sheet or web to dissipate to ground. If the conductivity is sufficiently high, charge cannot accumulate on the sheet [10], although, as the speed of the sheet increases, charging occurs above a critical speed [7]. Sheet resistivity is a property of the coated layer and measurement methods have been reported to characterize the consequences of resistivity; charge decay [11], charge dissipation [12], and electric field shielding performance of conductive sheets [13].

If the conductivity is constant, i.e., independent of electric field, charge relaxation is exponential in time and is characterized by a time constant  $\tau^e$  [14, Sec. 7.2, p.372]. For moving webs and sheets, charge dissipates when charge relaxation occurs quickly relative to the mechanical transport time. The ratio of the charge relaxation time  $\tau^e$  to the mechanical transport time  $\tau^m$  is the electric Reynolds number  $R_e$  [14, Sec. 7.2, p.383]

$$R_e = \frac{\tau^e}{\tau^m}. \quad (1)$$

When conductivity is sufficient for charge to dissipate quickly, the electric Reynolds number is small compared with unity. Based on a simple dimensional analysis, the charge relaxation time for a sheet in free space may be estimated to be

$$\tau^e = \frac{\varepsilon_0 L}{\sigma_s} \quad (2)$$

where  $\sigma_s$  is the sheet conductivity,  $\varepsilon_0$  is the permittivity of free space, and  $L$  is a characteristic length, taken to be the length of the sheet. The electric Reynolds number can be written

$$R_e = \frac{\varepsilon_0 L U}{\sigma_s L} = \frac{\varepsilon_0 U}{\sigma_s} = \varepsilon_0 \rho_s U \quad (3)$$

where  $U$  is the sheet speed and  $\rho_s$  is the sheet resistivity. The product of resistivity and speed is a useful scaling factor [6]. Using (3), the boundary between charging and no charging resulting from a model computation [10] is found to be approximately

$$R_e = \frac{\varepsilon_0 U}{\sigma_s} \approx \frac{1}{100}. \quad (4)$$

In later work, results of this model computation were confirmed experimentally [7] where the boundary between charging and no charging was found to be

$$R_e = \frac{\varepsilon_0 U}{\sigma_s} = \frac{\varepsilon_0 \left( \frac{1 \text{ m}}{s} \right)}{(6 \times 10^{-10} \Omega^{-1})} \approx \frac{1}{100}. \quad (5)$$

In the early work on motion picture films [6], a transition in the discharging constant from high to low discharging occurs at approximately

$$R_e = \frac{\varepsilon_0 U}{\sigma_s} = \varepsilon_0 \left( 10^{11} \Omega - \frac{m}{s} \right) \approx 1. \quad (6)$$

Using a simple estimate for the electrical relaxation time (2), the critical electric Reynolds number that identifies the onset of web charging varies from 0.01 in (5) to 1 in (6). One possible explanation of this  $100 \times$  difference is that the simple dimensional analysis to estimate the electrical relaxation time is missing key information.

### C. Geometry Affects Charge Relaxation

While conductivity is a material property, charge relaxation is influenced by geometry because the electric fields driving conduction depend on geometry. The influence of geometry on the electric fields near a charged sheet has been analyzed [15]–[18]. The effect of geometry on charge relaxation in (2) is clear because the charge relaxation time is estimated to be proportional to the length of the sheet. For the more complex geometry of a charge sheet suspended between conveyance rollers, charge relaxation is found to vary with the span length [19].

Charge relaxation in a partially filled vessel is closely related to web charge dissipation because a nearby grounded conductor slows charge relaxation in both cases. Charge relaxation in partially filled vessels has been extensively analyzed [20]–[22]. The decay of electrostatic charge is prolonged significantly by capacitive coupling between the free surface of the stored material to the vessel walls [20]. If the vessel has an insulating liner, charge accumulates on the surface of the liner and dissipates very slowly due to capacitive coupling through the liner [21]. Conductivity along the free surface in a partially filled vessel affects charge decay in a complex way though capacitive coupling to the walls slows charge dissipation [22].

The key experimental result (5) is that web charge dissipates when the charge relaxation time is sufficiently short. To understand this result, and generalize it to other geometries, the ef-

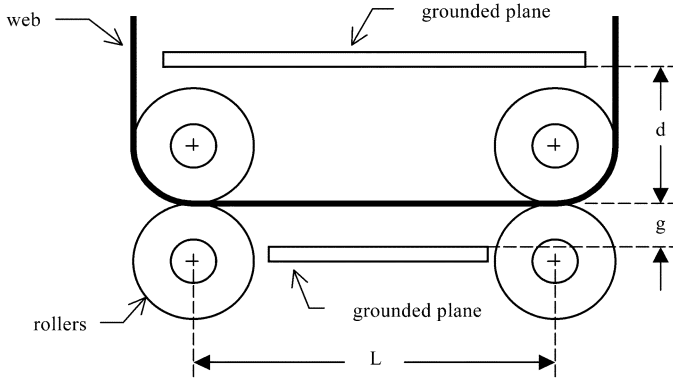


Fig. 1. Physical geometry of a web or sheet suspended between conveyance rollers.

fect of the geometry on charge relaxation must be known. Here, the analysis of a sheet suspended between conveyance rollers [15], [19] has been extended to include the effects of a nearby grounded, conducting plane. The charge relaxation time is found to increase as the distance to the grounded plane decreases. Charge relaxation is slowed because the tangential electric field need to drive surface current becomes smaller as the distance to the grounded plane decreases. When the insulating sheet is resting on the grounded plane, the electric field is nearly normal to the surface, and the charge relaxation time increases dramatically

$$\tau^e = \frac{\varepsilon_1 L^2}{\pi^2 \sigma_s g} = \frac{\varepsilon_0 L}{\sigma_s} \left( \frac{\varepsilon_1}{\varepsilon_0} \right) \left( \frac{L}{\pi^2 g} \right), \quad g \ll L. \quad (7)$$

$L$  is the span length,  $g$  is the thickness of the sheet, and  $\varepsilon_1$  is the electric permittivity of the web material.

## II. ANALYSIS

### A. Idealized Model

Shown in Fig. 1 is a physical geometry that represents a typical part of the conveyance path in an industrial process or in consumer equipment. A continuous web or a cut sheet is suspended rigidly between conveyance rollers. The rollers are grounded conductors. Rarely are the rollers the only grounded objects near the web. The grounded planes on either side of the web represent grounded conductors such as the machine frame, machine panels or baffles, or the floor. In the limit that  $g$  becomes very small relative to  $L$ , the grounded plane beneath the sheet represents the receiving tray or sorter bins at the output of a printer or copier.

The electric potential is a solution of the Laplace equation

$$\frac{\partial^2 \Phi}{\partial x^2} + \frac{\partial^2 \Phi}{\partial z^2} = 0. \quad (8)$$

There is no known, closed-form solution for the electric potential for the web-roller geometry illustrated in Fig. 1. Following the ideas of Nickell and Taylor [15], an idealization of this web-roller geometry is shown in Fig. 2. While the electric potential in the immediate vicinity of the roller nips will be crudely approximated in this idealization, the effects of the grounded planes will be well represented.

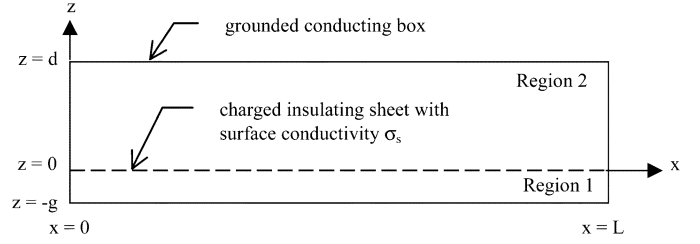


Fig. 2. Idealized web-roller geometry.

The solution for the electric potential  $\Phi(x, y)$  by separation of variables is given in the Appendix. The expressions for  $\Phi(x, y)$  for an initially uniform charge distribution are

$$\Phi_1(x, z, t) = \left( \frac{4\rho_{s,0}L}{\pi^2 \varepsilon_0} \right) \sum_{n \in \text{odd}} \left( \frac{1}{n^2} \right) \times \left[ \frac{\cosh(n\pi \frac{d}{L}) \sin(n\pi \frac{x}{L})}{\frac{\varepsilon_1}{\varepsilon_0} \tanh(n\pi \frac{d}{L}) + \frac{\varepsilon_2}{\varepsilon_0} \tanh(n\pi \frac{d}{L})} \right] \times \left[ \frac{\cosh(n\pi \frac{z}{L})}{\cosh(n\pi \frac{d}{L})} + \frac{\sinh(n\pi \frac{z}{L})}{\sinh(n\pi \frac{d}{L})} \right] e^{-t/\tau_n}, \quad -g \leq z \leq 0 \quad (9)$$

$$\Phi_2(x, z, t) = \left( \frac{4\rho_{s,0}L}{\pi^2 \varepsilon_0} \right) \sum_{n \in \text{odd}} \left( \frac{1}{n^2} \right) \times \left[ \frac{\cosh(n\pi \frac{d}{L}) \sin(n\pi \frac{x}{L})}{\frac{\varepsilon_1}{\varepsilon_0} \tanh(n\pi \frac{d}{L}) + \frac{\varepsilon_2}{\varepsilon_0} \tanh(n\pi \frac{d}{L})} \right] \times \left[ \frac{\cosh(n\pi \frac{z}{L})}{\cosh(n\pi \frac{d}{L})} - \frac{\sinh(n\pi \frac{z}{L})}{\sinh(n\pi \frac{d}{L})} \right] e^{-t/\tau_n}, \quad 0 \leq z \leq d \quad (10)$$

where the time constant  $\tau_n$  is

$$\tau_n = \frac{\varepsilon_0 L}{n\pi \sigma_s} \left[ \frac{\varepsilon_1}{\varepsilon_0} \tanh(n\pi \frac{d}{L}) + \frac{\varepsilon_2}{\varepsilon_0} \tanh(n\pi \frac{d}{L}) \right]. \quad (11)$$

## III. RESULTS

### A. Comparison With the Result of Nickell and Taylor

Nickell and Taylor [15] solved the problem for  $\varepsilon_1 = \varepsilon_2 = \varepsilon_0$ ,  $L = 1$  m, and the grounded planes are far away,  $g, d \gg L$ . For this case, the expressions (9) and (10) for the electric potential at  $t = 0$  simplify to

$$\Phi_1(x, z, t = 0) = \left( \frac{2\rho_{s,0}L}{\pi^2 \varepsilon_0} \right) \sum_{n \in \text{odd}} \left( \frac{1}{n^2} \right) \times \sin\left(n\pi \frac{x}{L}\right) e^{+(n\pi(z/L))}, \quad -\infty < z \leq 0 \quad (12)$$

$$\Phi_2(x, z, t = 0) = \left( \frac{2\rho_{s,0}L}{\pi^2 \varepsilon_0} \right) \sum_{n \in \text{odd}} \left( \frac{1}{n^2} \right) \times \sin\left(n\pi \frac{x}{L}\right) e^{-(n\pi(z/L))}, \quad 0 \leq z < \infty \quad (13)$$

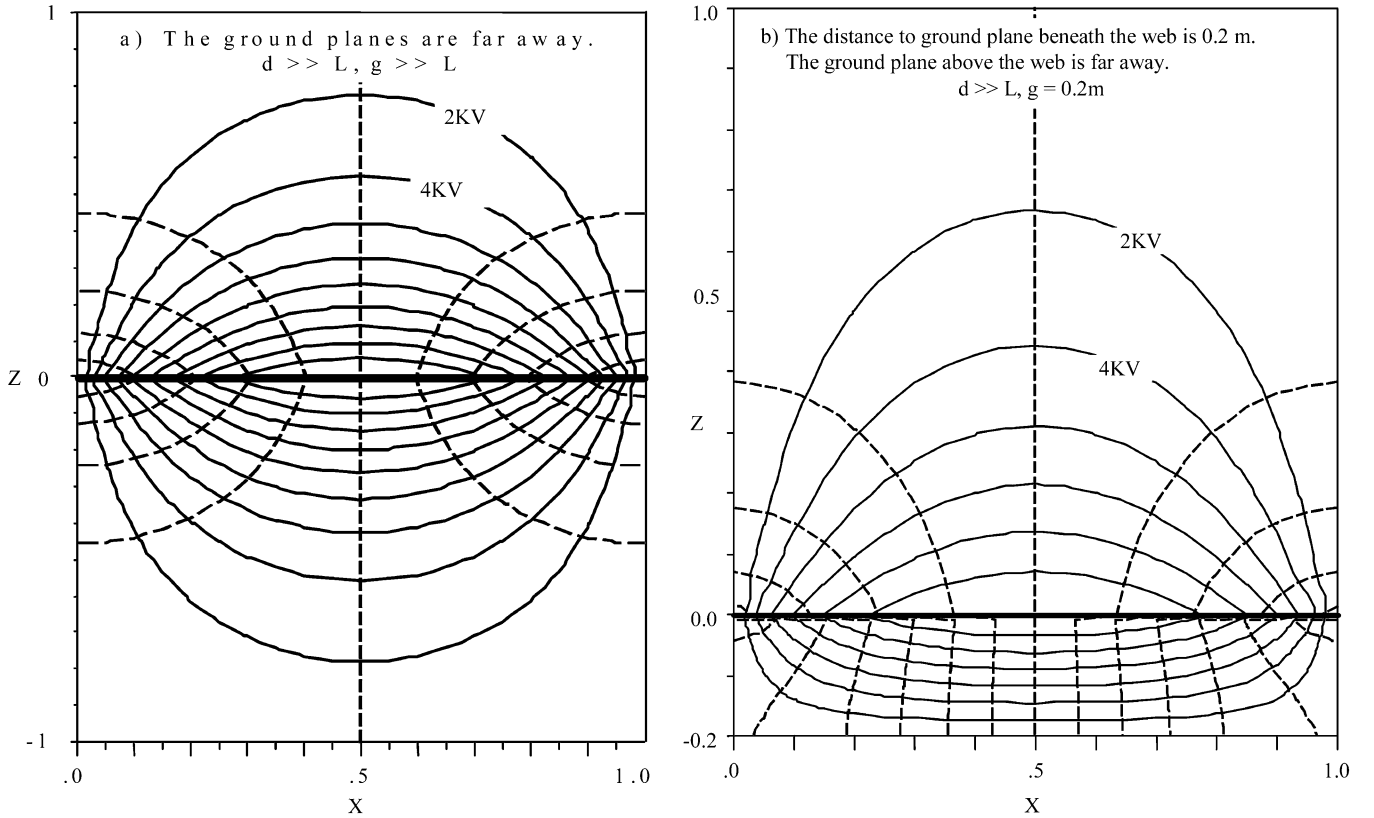


Fig. 3. Equipotentials and electric fields for  $L = 1$  m and an initial charge distribution of  $1$  ( $\mu\text{C}/\text{m}^2$ ).

which are consistent with the results previously reported. Fig. 3(a) illustrates the equipotentials and electric field lines using the stream function given by (A24) and (A25) for a surface charge density of  $1$  ( $\mu\text{C}/\text{m}^2$ ). The equipotentials are plotted at increments of  $2$  kV. The maximum voltage of  $21.0$  kV is midway along the web surface as reported by Nickell and Taylor [15]. Note also that the electric field along the surface of the web has a significant tangential component, i.e., there is a significant electric field at the web surface that is parallel to the surface. This field drives surface currents that speed charge relaxation. Later, when the case of a grounded plane close to the web is considered, the electric field will be nearly normal to the surface, reducing surface currents and slowing charge relaxation.

### B. Comparison With the Result of Pazda

Pazda [19] solved for the time-dependent potential due to charge relaxation for the case when  $\varepsilon_1 = \varepsilon_2 = \varepsilon_0$  and when the grounded planes are far away:  $g, d \gg L$ . For this case, the expressions for the electric potential (9) and (10) simplify to

$$\Phi_1(x, z, t) = \left( \frac{2\rho_{s,0}L}{\pi^2\varepsilon_0} \right) \sum_{n \in \text{odd}} \left( \frac{1}{n^2} \right) \times \sin\left(n\pi \frac{x}{L}\right) e^{n\pi(z/L)} e^{-(t/\tau_n)}, \quad -\infty < z \leq 0 \quad (14)$$

$$\Phi_2(x, z, t) = \left( \frac{2\rho_{s,0}L}{\pi^2\varepsilon_0} \right) \sum_{n \in \text{odd}} \left( \frac{1}{n^2} \right) \times \sin\left(n\pi \frac{x}{L}\right) e^{-n\pi(z/L)} e^{-(t/\tau_n)}, \quad 0 \leq z < \infty \quad (15)$$

where the time constant  $\tau_n$  is given by

$$\tau_n = \frac{2\varepsilon_0 L}{n\pi\sigma_s} \equiv \frac{2\varepsilon_0}{\sigma_s \alpha_n}. \quad (16)$$

The eigenvalues  $\alpha_n$  referred to in [19] are given by

$$\alpha_n = \frac{n\pi}{L}. \quad (17)$$

These results are consistent with those previously reported by Pazda [19].

### C. A Nearby, Grounded Plane ( $g \approx L$ ) Affects the Potential, Electric Field, and Charge Relaxation

When a grounded plane is near the web, the electric potential is reduced and the electric fields become more normal to the web surface. Fig. 3(b) shows a plot of the potential and electric field for the case where  $\varepsilon_1 = \varepsilon_2 = \varepsilon_0$ ,  $L = 1$  m, the grounded plane beneath the web is  $0.2$  m away, and the sheet has an initial charge density of  $1$  ( $\mu\text{C}/\text{m}^2$ ).

The fundamental charge relaxation time is the leading term in (11) where  $n = 1$ .

$$\tau^e = \frac{\varepsilon_0 L}{\pi\sigma_s} \left[ \frac{1}{\tanh\left(\pi \frac{g}{L}\right)} + 1 \right]. \quad (18)$$

Note that the charge relaxation time  $\tau^e$  increases as  $g$  decreases.

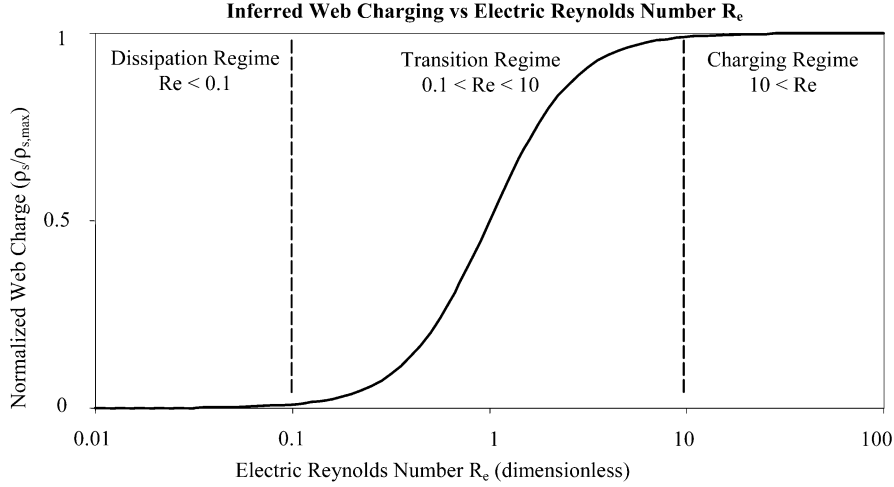


Fig. 4. Expected variation of web charge as a function of the electric Reynolds number  $R_e$ .

#### D. An Insulating Sheet Resting on the Grounded Plane ( $g \ll L$ )

Consider the case where the surface of a sheet away from the grounded plane has finite surface conductivity  $\sigma_s$ . This physical geometry may be analyzed by identifying dimension  $g$  as the thickness of the sheet, which is very small compared with the span length  $L$ . For this case, the fundamental charge relaxation time, the leading term in (11) where  $n = 1$  is

$$\tau^e = \frac{\varepsilon_0 L^2}{\pi^2 \sigma_s g} \left( \frac{\varepsilon_1}{\varepsilon_0} \right) = \frac{\varepsilon_0 L}{\sigma_s} \left( \frac{\varepsilon_1}{\varepsilon_0} \right) \left( \frac{L}{\pi^2 g} \right). \quad (19)$$

Note that the estimate of the charge relaxation time based on a simple dimensional analysis (2) severely underestimates the actual charge relaxation time by a factor of  $(\varepsilon_1/\varepsilon_0)(L/\pi^2 g)$ .

### IV. DISCUSSION

#### A. Geometry Affects Charge Relaxation

Charge relaxation depends both on the surface conductivity of the web and the geometry. A nearby, grounded surface can greatly increase the charge relaxation time. Estimating the charge relaxation time using a simple dimensional analysis,  $R_e = 0.01$  is found in (4) to be the boundary between charging and no charging resulting from a model computation [10]. The geometry for this model computation is an insulating sheet distance  $H$  away from a grounded plane. While the details of the model computation are not completely given in [10], it is reasonable to conclude that the charge relaxation time is much longer than the value estimated in (2). For example, using (19) the electric Reynolds number is estimated to be

$$\begin{aligned} R_e &= \frac{\tau^e}{\tau^m} = \frac{\varepsilon_0 L}{\sigma_s} \left( \frac{\varepsilon_1}{\varepsilon_0} \right) \left( \frac{L}{\pi^2 H} \right) \left( \frac{U}{L} \right) \\ &= \frac{\varepsilon_0 U}{\sigma_s} \left( \frac{\varepsilon_1}{\varepsilon_0} \right) \left( \frac{L}{\pi^2 H} \right) \approx \left( \frac{1}{100} \right) (1) \left( \frac{1 \text{ m}}{\pi^2 \times 0.01 \text{ m}} \right) \\ &\cong 0.1 \end{aligned} \quad (20)$$

where the sheet length  $L$  is taken to be 1 m, and the distance  $H$ , analogous to dimension  $g$  in (19), is 10 mm. While the actual values for the computation are not known, the conclusion is that  $R_e$  is likely much larger than 0.01.

Because charge relaxation is exponential in time, the transition from no charging to charging is inferred to have the characteristics illustrated in Fig. 4.

When charge relaxation is fast relative to the mechanical transport time, charge dissipates quickly and little or no charge accumulates. In this “Dissipation Regime,” the no charging behavior is independent of conductivity and speed. When charge relaxation is slow relative to the mechanical transport time, charge accumulates on the web surface. Because dissipation is negligible in this “Charging Regime,” surface conductivity and speed are of little consequence. Between these limits is a “Transition Regime” where charge relaxation and convective charge transport are both important. Some charge accumulates and the dynamics depend strongly on both conductivity and speed.

#### B. Limitations

The geometry analyzed here is an idealized geometry. The electric fields near the roller contacts are only crudely approximated by this geometry. It is reasonable to expect that the actual charge relaxation time is longer than the results reported here. The electric fields along the web near the rollers are nearly normal to the web surface in contrast to the fields shown in Fig. 3(a) that are nearly tangential to the web surface for  $x \approx 0$  and  $x \approx 1$ .

### V. CONCLUSION

The analysis of a sheet suspended between conveyance rollers [15], [19] has been extended to include the effects of a nearby, grounded plane. The charge relaxation time is found to increase as the distances to the grounded planes  $g$  and  $d$  decrease

$$\tau^e = \frac{\varepsilon_0 L}{\pi \sigma_s} \left[ \frac{\frac{\varepsilon_1}{\varepsilon_0}}{\tanh(\pi \frac{g}{L})} + \frac{\frac{\varepsilon_2}{\varepsilon_0}}{\tanh(\pi \frac{d}{L})} \right]. \quad (21)$$

When the grounded planes are far away ( $d, g \gg L$ ), the electric potentials (9) and (10) are consistent with the analysis of Nickell and Taylor [15]. The charge relaxation time (11) is consistent with the work by Pazda [19].

When the grounded planes are near ( $d, g \cong L$ ), charge relaxation is slowed because the tangential electric field need to drive

surface current becomes smaller. When the insulating sheet is resting on a grounded plane ( $g \ll L, d \gg L$ ), the electric field is nearly normal to the surface. The charge relaxation time increases greatly

$$\tau^e = \frac{\varepsilon_0 L^2}{\pi^2 \sigma_s g} \left( \frac{\varepsilon_1}{\varepsilon_0} \right) = \frac{\varepsilon_0 L}{\sigma_s} \left( \frac{\varepsilon_1}{\varepsilon_0} \right) \left( \frac{L}{\pi^2 g} \right), \quad g \ll L; \quad d \gg L. \quad (22)$$

Inferred from this analysis is the dependence of charging on the electric Reynolds number that can be divided into three regimes: dissipation ( $R_e < 0.1$ ), transition ( $0.1 < R_e < 10$ ), and charging ( $10 < R_e$ ). While the evidence for this three-regime model is limited, it is consistent with previous results [7], [10].

## APPENDIX

### A. Potential Solution by Separation of Variables

Using separation of variables, the electric potential  $\Phi(x, y)$  has the form [23]

$$\begin{aligned} \Phi(x, z) = & (P + Rx + Sz + Txz) \\ & + [A \sin(\alpha x) + B \cos(\alpha x)] \\ & \times [C \sinh(\alpha z) + D \cosh(\alpha z)] \end{aligned} \quad (A1)$$

where  $\alpha$  is a constant. The potential (A1) is valid for charge-free regions, so separate expressions for the potential must be used for the regions below and above the charged web identified as region 1 and region 2 respectively in Fig. 2. The 16 constants must be chosen to satisfy the boundary conditions. In both regions, the potential must be zero at each corner of the grounded box. Clearly, constants  $P$ ,  $R$ ,  $S$ , and  $T$  must be zero in both regions.

The potential must be zero along the  $x = 0$  boundary in both regions

$$B_1 = B_2 = 0. \quad (A2)$$

The potential must be zero along the  $x = L$  boundary in both regions

$$\sin(\alpha L) = 0. \quad (A3)$$

The sine function has zeros at integral multiples of  $\pi$ , so the constant  $\alpha$  must be

$$\alpha = \frac{n\pi}{L} \quad (A4)$$

where  $n$  is an integer in the range  $(1, \infty)$ . For  $n = 0$ , the potential is zero everywhere and provides no information in this analysis. The expression (A1) for the potential  $\Phi(x, y)$  can now be written

$$\begin{aligned} \Phi_1(x, z) = & \sum_{n=1}^{\infty} \sin\left(n\pi \frac{x}{L}\right) \\ & \times \left[ C_1 \sinh\left(n\pi \frac{z}{L}\right) + D_1 \cosh\left(n\pi \frac{z}{L}\right) \right], \\ & -g < z < 0 \end{aligned} \quad (A5)$$

$$\begin{aligned} \Phi_2(x, z) = & \sum_{n=1}^{\infty} \sin\left(n\pi \frac{x}{L}\right) \\ & \times \left[ C_2 \sinh\left(n\pi \frac{z}{L}\right) + D_2 \cosh\left(n\pi \frac{z}{L}\right) \right], \\ & 0 < z < d \end{aligned} \quad (A6)$$

where coefficient  $A_1$  and  $A_2$  have been set to unity without loss of generality. In region 1, the potential must be zero along the  $z = -g$  boundary, and (A5) becomes

$$\begin{aligned} \Phi_1(x, z) = & \sum_{n=1}^{\infty} C'_1 \sin\left(n\pi \frac{x}{L}\right) \\ & \times \left[ \frac{\sinh\left(n\pi \frac{z}{L}\right)}{\sinh\left(n\pi \frac{g}{L}\right)} + \frac{\cosh\left(n\pi \frac{z}{L}\right)}{\cosh\left(n\pi \frac{g}{L}\right)} \right], \\ & -g \leq z < 0. \end{aligned} \quad (A7)$$

Similarly, in region 2, the potential must be zero along the  $z = d$  boundary and (A8) becomes

$$\begin{aligned} \Phi_2(x, z) = & \sum_{n=1}^{\infty} C'_2 \sin\left(n\pi \frac{x}{L}\right) \\ & \times \left[ \frac{\sinh\left(n\pi \frac{z}{L}\right)}{\sinh\left(n\pi \frac{d}{L}\right)} - \frac{\cosh\left(n\pi \frac{z}{L}\right)}{\cosh\left(n\pi \frac{d}{L}\right)} \right], \\ & 0 < z \leq d. \end{aligned} \quad (A8)$$

Note that constants  $C'_1$  and  $C'_2$  contain  $C_1$  and  $C_2$  as well as additional constant terms. Across the charged web at the  $z = 0$  boundary, the potential must be continuous. The expressions for the potential can be written

$$\begin{aligned} \Phi_1(x, z) = & \sum_{n=1}^{\infty} \frac{C_1''}{\cosh\left(n\pi \frac{d}{L}\right)} \sin\left(n\pi \frac{x}{L}\right) \\ & \times \left[ \frac{\cosh\left(n\pi \frac{z}{L}\right)}{\cosh\left(n\pi \frac{d}{L}\right)} + \frac{\sinh\left(n\pi \frac{z}{L}\right)}{\sinh\left(n\pi \frac{d}{L}\right)} \right], \\ & -g \leq z \leq 0 \end{aligned} \quad (A9)$$

$$\begin{aligned} \Phi_2(x, z) = & \sum_{n=1}^{\infty} \frac{C_1''}{\cosh\left(n\pi \frac{d}{L}\right)} \sin\left(n\pi \frac{x}{L}\right) \\ & \times \left[ \frac{\cosh\left(n\pi \frac{z}{L}\right)}{\cosh\left(n\pi \frac{d}{L}\right)} + \frac{\sinh\left(n\pi \frac{z}{L}\right)}{\sinh\left(n\pi \frac{d}{L}\right)} \right], \\ & 0 \leq z \leq d. \end{aligned} \quad (A10)$$

The last boundary condition is that the electric field must satisfy Gauss' law across the charged web at the  $z = 0$  boundary

$$\varepsilon_2 E_{2,z} - \varepsilon_1 E_{1,z} = \rho_s(x, t). \quad (A11)$$

Using the potential expressions (A9) and (A10), and after some manipulation, (A11) can be written

$$\begin{aligned} \rho_s(x, t) = & \sum_{n=1}^{\infty} C_1'' \left( \frac{n\pi}{L} \right) \left[ \frac{\frac{\varepsilon_1}{\tanh\left(n\pi \frac{d}{L}\right)} + \frac{\varepsilon_2}{\tanh\left(n\pi \frac{d}{L}\right)}}{\cosh\left(n\pi \frac{d}{L}\right) \cosh\left(n\pi \frac{d}{L}\right)} \right] \\ & \times \sin\left(n\pi \frac{x}{L}\right). \end{aligned} \quad (A12)$$

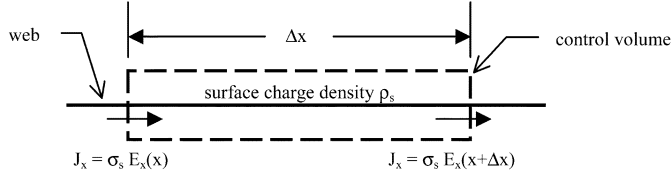


Fig. 5. Charge is conserved as current flows along the surface of the web.

### B. Conservation of Charge and Charge Relaxation

Because of surface conductivity, charge moves along the web surface. Fig. 5 illustrates charge conservation along the surface. From Fig. 5, charge conservation can be written

$$\Delta x \frac{\partial \rho_s}{\partial t} = \sigma_s E_x(x) - \sigma_s E_x(x + \Delta x). \quad (\text{A13})$$

Using the expression (A9) for the potential in region 1, charge conservation can be written

$$\frac{\partial \rho_s}{\partial t} + \sum_{n=1}^{\infty} C''_1 \sigma_s \left( \frac{n\pi}{L} \right)^2 \left[ \frac{\sin(n\pi \frac{x}{L})}{\cosh(n\pi \frac{d}{L}) \cosh(n\pi \frac{d}{L})} \right] = 0. \quad (\text{A14})$$

Using the expression (A14) for charge conservation, Gauss' law as expressed by (A12) can be written

$$\frac{\partial C''_1}{\partial t} + \frac{C''_1}{\tau_n} = 0 \quad (\text{A15})$$

where

$$\tau_n = \frac{\varepsilon_0 L}{n\pi \sigma_s} \left[ \frac{\varepsilon_1}{\varepsilon_0} + \frac{\varepsilon_2}{\varepsilon_0} \right]. \quad (\text{A16})$$

The expression (A12) for surface charge density can now be written

$$\rho_s(x, t) = \sum_{n=1}^{\infty} C''_{1,0} \left( \frac{n\pi}{L} \right) \left[ \frac{\frac{\varepsilon_1}{\varepsilon_0} + \frac{\varepsilon_2}{\varepsilon_0}}{\cosh(n\pi \frac{d}{L}) \cosh(n\pi \frac{d}{L})} \right] \times \sin\left(n\pi \frac{x}{L}\right) e^{-t/\tau_n} \quad (\text{A17})$$

where  $C''_{1,0}$  is the initial value of  $C''_1$  at  $t = 0$  and  $\tau_n$  is given by (A16). Taking the case where the initial surface charge density is uniform, the expression for  $C''_{1,0}$  surface charge density is

$$C''_{1,0} = \begin{cases} \left( \frac{4\rho_{s,0}L}{(n\pi)^2} \right) \left[ \frac{\cosh(n\pi \frac{d}{L}) \cosh(n\pi \frac{d}{L})}{\frac{\varepsilon_1}{\varepsilon_0} + \frac{\varepsilon_2}{\varepsilon_0}} \right], & n \in \text{odd} = 0; \\ n \in \text{even}. & \end{cases} \quad (\text{A18})$$

### C. Analysis Summary and Electric Field Stream Function

The expressions for electric potential given by (A9) and (A10) for the case of uniform initial charge distribution are

$$\Phi_1(x, z, t) = \left( \frac{4\rho_{s,0}L}{\pi^2 \varepsilon_0} \right) \sum_{n \in \text{odd}} \left( \frac{1}{n^2} \right) \times \left[ \frac{\cosh(n\pi \frac{d}{L}) \sin(n\pi \frac{x}{L})}{\frac{\varepsilon_1}{\varepsilon_0} + \frac{\varepsilon_2}{\varepsilon_0}} \right] \times \left[ \frac{\cosh(n\pi \frac{z}{L})}{\cosh(n\pi \frac{d}{L})} + \frac{\sinh(n\pi \frac{z}{L})}{\sinh(n\pi \frac{d}{L})} \right] e^{-t/\tau_n}, \quad -g \leq z \leq 0 \quad (\text{A19})$$

$$\Phi_2(x, z, t) = \left( \frac{4\rho_{s,0}L}{\pi^2 \varepsilon_0} \right) \sum_{n \in \text{odd}} \left( \frac{1}{n^2} \right) \times \left[ \frac{\cosh(n\pi \frac{d}{L}) \sin(n\pi \frac{x}{L})}{\frac{\varepsilon_1}{\varepsilon_0} + \frac{\varepsilon_2}{\varepsilon_0}} \right] \times \left[ \frac{\cosh(n\pi \frac{z}{L})}{\cosh(n\pi \frac{d}{L})} - \frac{\sinh(n\pi \frac{z}{L})}{\sinh(n\pi \frac{d}{L})} \right] e^{-t/\tau_n}, \quad 0 \leq z \leq d \quad (\text{A20})$$

and, the expression for the surface charge density is

$$\rho_s(x, t) = \left( \frac{4\rho_{s,0}}{\pi} \right) \sum_{n \in \text{odd}} \frac{1}{n} \sin\left(n\pi \frac{x}{L}\right) e^{-t/\tau_n} \quad (\text{A21})$$

where

$$\tau_n = \frac{\varepsilon_0 L}{n\pi \sigma_s} \left[ \frac{\varepsilon_1}{\varepsilon_0} + \frac{\varepsilon_2}{\varepsilon_0} \right]. \quad (\text{A22})$$

The stream function  $\Psi(x, z, t)$  provides a map of the electric field and can be constructed using the Cauchy–Riemann conditions [24]

$$\frac{\partial \Psi}{\partial x} = \frac{\partial \Phi}{\partial z}, \quad \frac{\partial \Psi}{\partial z} = -\frac{\partial \Phi}{\partial x}. \quad (\text{A23})$$

The expressions for the stream function are

$$\Psi_1(x, y, t) = \left( \frac{4\rho_{s,0}L}{\pi^2 \varepsilon_0} \right) \sum_{n \in \text{odd}} \left( \frac{1}{n^2} \right) \times \left[ \frac{\cosh(n\pi \frac{d}{L}) \cos(n\pi \frac{x}{L})}{\frac{\varepsilon_1}{\varepsilon_0} + \frac{\varepsilon_2}{\varepsilon_0}} \right] \times \left[ \frac{\sinh(n\pi \frac{z}{L})}{\cosh(n\pi \frac{d}{L})} + \frac{\cosh(n\pi \frac{z}{L})}{\sinh(n\pi \frac{d}{L})} \right] \times e^{-t/\tau_n} \quad (\text{A24})$$

$$\Psi_2(x, z, t) = \left( \frac{4\rho_{s,0}L}{\pi^2 \varepsilon_0} \right) \sum_{n \in \text{odd}} \left( \frac{1}{n^2} \right) \times \left[ \frac{\cosh(n\pi \frac{d}{L}) \cos(n\pi \frac{x}{L})}{\frac{\varepsilon_1}{\varepsilon_0} + \frac{\varepsilon_2}{\varepsilon_0}} \right] \times \left[ \frac{\sin(n\pi \frac{z}{L})}{\cosh(n\pi \frac{d}{L})} + \frac{\cosh(n\pi \frac{z}{L})}{\sinh(n\pi \frac{d}{L})} \right] \times e^{-t/\tau_n}. \quad (\text{A25})$$

### REFERENCES

- [1] H. W. Cleveland, "A method of measuring electrification of motion picture film applied to cleaning operations," *J. SMPTE*, vol. 55, pp. 37–44, 1950.
- [2] R. G. Cunningham and T. J. Coburn, "Charge growth equation for belts of insulating materials passing over grounded rollers," *J. Appl. Phys.*, vol. 37, no. 8, pp. 2931–2935, 1966.
- [3] E. Kramp, "Charge generation of photographic film by roller contact," *J. Electrostat.*, vol. 30, pp. 3–16, 1993.
- [4] K. L. Clum, "Analytical representation of web-roller electrification," in *Inst. Phys. Conf Ser.*, 1979, pp. 27–36.

- [5] R. J. Pazda and K. Clum, "Electrification analysis of a web or sheet moving between pinch rollers," *J. Electrostat.*, vol. 35, pp. 191–202, 1995.
- [6] K. L. Clum, H. R. McNair, and J. Pytlak, "Static control in film transport systems," *J. SMPTE*, pp. 636–638, July 1984.
- [7] J. F. Hughes, A. M. K. Au, and A. R. Blythe, "Electrical charging and discharging between films and metal rollers," in *Inst. Phys. Conf. Ser.*, 1979, pp. 37–44.
- [8] M. Zaretsky, "Some electrostatic design issues for a thermal receiver," *J. Electrostat.*, vol. 46, pp. 221–230, 1999.
- [9] M. N. Horenstein and N. Roberts, "Peeling force for an electrostatically charged sheet on a grounded surface," *J. Electrostat.*, vol. 35, pp. 179–190, 1995.
- [10] T. Horvath and I. Berta, "Mathematical simulation of electrostatic hazards," in *Inst. Phys. Conf. Ser.*, 1975, pp. 256–263.
- [11] N. Jonassen, I. Hansson, and A. R. Nielsen, "On the correlation between decay of charge and resistance parameters of sheet materials," in *Inst. Phys. Conf. Ser.*, 1979, pp. 215–244.
- [12] J. N. Chubb, J. Harbour, and P. Domenichini, "Instrumentation for on-line measurement of the charge dissipation capabilities of web and coated film materials," in *Inst. Phys. Conf. Ser.*, 1991, pp. 153–258.
- [13] E. Kramp and J. P. Ansermet, "The AC field window method—An unequivocal technique to characterize the static behavior of photographic films," *J. Electrostat.*, vol. 30, pp. 315–326, 1993.
- [14] H. H. Woodson and J. R. Melcher, *Electromechanical Dynamics (Part II)*. New York: Wiley, 1968.
- [15] R. M. Nickell and D. M. Taylor, "Electric fields and potentials in the vicinity of electrostatically charged sheet product suspended between two earthed boundaries," *J. Electrostat.*, vol. 26, pp. 235–243, 1991.
- [16] M. N. Horenstein, "Measuring isolated surface charge with a noncontacting voltmeter," *J. Electrostat.*, vol. 35, pp. 203–213, 1995.
- [17] W. J. Durkin, "Dangers in interpreting electrostatic measurements on plastic webs," *J. Electrostat.*, vol. 35, pp. 215–229, 1995.
- [18] A. E. Seaver, "Analysis of electrostatic measurements on nonconducting webs," *J. Electrostat.*, vol. 35, pp. 231–243, 1995.
- [19] R. J. Pazda, "Surface charge relaxation on a sheet located between grounded rollers," *J. Electrostat.*, vol. 37, pp. 21–28, 1996.
- [20] T. B. Jones and S. Chen, "Charge relaxation in partially filled vessels," *J. Electrostat.*, vol. 22, pp. 185–197, 1989.
- [21] —, "Charge relaxation in vessels with insulating liners," *J. Electrostat.*, vol. 22, pp. 199–212, 1989.
- [22] R. J. Pazda and T. B. Jones, "Effect of surface conduction on charge relaxation in partially filled vessels," *J. Electrostat.*, vol. 28, pp. 175–185, 1992.
- [23] H. A. Hass and J. R. Melcher, *Electromagnetic Fields and Energy*. Englewood Cliffs, NJ: Prentice-Hall, 1989, sec. 5.4, p. 152.
- [24] G. Arfken, *Mathematical Methods for Physicists*, 2nd ed. New York: Academic, 1970, sec. 6.2, p. 303.



**Kelly Robinson** (M'78–SM'90) received the M.S. degree from the University of Illinois, Urbana, in 1978, and the Ph.D. degree from Colorado State University, Fort Collins, in 1982, both in electrical engineering.

In 1982, he joined Eastman Kodak Company, Rochester, NY, and worked on electrophotographic copier technology. In 1997, he became the Unit Director of the Eastman Kodak Surface Modification and Electrostatic Unit, where he was responsible for the technical strategy and leadership of research and

development projects involving vacuum coating, plasma processes, and electrostatic technologies. Currently, he is a Research Scientist and Electrostatics Group Leader with the principal responsibility of designing products and manufacturing processes to minimize electrostatic difficulties. His technical interests are centered on applications and theory of electrostatic technology, including electric forces, charging particles, corona ionization, and high-voltage engineering. He is the holder of nine U.S. patents on copier technology and the design of roll-to-roll manufactured products for static protection. He is active professionally in promoting technical progress in electrostatic technologies and the career interests of those working in the field.

Dr. Robinson served as Chairman of the Electrostatic Processes Committee of the IEEE Industry Applications Society (IAS-EPC) during 1987–1988, and is currently Vice-President of the Electrostatics Society of America. He worked to establish the IAS-EPC prize paper award for "Creativity and Innovation" and has served since 2000 on the James R. Melcher Prize Paper Award Selection Committee. In 2003, he joined the Adjunct Faculty of the University of Arkansas at Little Rock, serving on a Ph.D. committee. He is a regular reviewer for the IEEE TRANSACTIONS ON INDUSTRY APPLICATIONS and the *Journal of Electrostatics*. He is a Member of the Electrostatics Society of America and the Sigma Xi Scientific Research Society.